VOLCANOLOGY

Rapid cooling and cold storage in a silicic magma reservoir recorded in individual crystals

Allison E. Rubin,[1]* Kari M. Cooper,[1]*† Christy B. Till,[2] Adam J. R. Kent,[3] Fidel Costa,[4,5] Maitrayee Bose,[2] Darren Gravley,[6] Chad Deering,[7] Jim Cole[6]

Silicic volcanic eruptions pose considerable hazards, yet the processes leading to these eruptions remain poorly known. A missing link is knowledge of the thermal history of magma feeding such eruptions, which largely controls crystallinity and therefore eruptability. We have determined the thermal history of individual zircon crystals from an eruption of the Taupo Volcanic Zone, New Zealand. Results show that although zircons resided in the magmatic system for 10^3 to 10^5 years, they experienced temperatures >650° to 750°C for only years to centuries. This implies near-solidus long-term crystal storage, punctuated by rapid heating and cooling. Reconciling these data with existing models of magma storage requires considering multiple small intrusions and multiple spatial scales, and our approach can help to quantify heat input to and output from magma reservoirs.

Understanding the chemical and physical evolution and the mobilization processes of magma stored in the crust at large, active silicic volcanic centers is critical for determining their hazard potential. A long-standing debate has focused on whether only a small (or negligible) volume of melt-rich magma exists at any given time, requiring further remobilization to erupt, or whether magma bodies are largely liquid for long periods of time (*1*–*9*). A critical part of this debate is the thermal balance, which is controlled by the amount and rate of magma added to the crust versus conductive cooling and the advective heat loss associated with eruption. Quantifying how thermal conditions vary within a magma reservoir and evolve over time is necessary for defining where and for how long bodies of magma are stored before eruptions. Numerical experiments can provide insight into the conditions under which melt-rich bodies can be sustained within the crust [e.g., (*1, 4, 10*)], but observational data on the long-term thermal conditions of magma storage are sparse, and those available to date average information from many crystals (*5*).

We present a geochemical approach to constraining the thermal history of individual zircon crystals in erupted magmas. We combined in situ ^{238}U-^{230}Th dating of zones within single crystals, yielding both the absolute ages of crystallization and the duration of crystal residence, with diffusion chronometry of Li concentration profiles from the same crystals to resolve temperature-dependent diffusion durations. Using this approach, we documented the thermal histories of seven individual zircon crystals from the Kaharoa eruption (0.7 thousand years ago, 5 km^3) of the Okataina Volcanic Centre (OVC) in the Taupo Volcanic Zone, New Zealand. These crystals have ages and trace element and Hf isotopic compositions that are typical of the much larger database of Kaharoa zircon measured previously (*11*–*13*). These seven crystals resided in the subsurface over tens to hundreds of thousands of years and directly sample conditions in the active reservoir that has fed OVC eruptions over this time, providing insights into the conditions of magma storage at one of the most active volcanic centers on the planet (*14*).

We measured ^{238}U-^{230}Th ages in two to four locations within each of the zircon crystals analyzed (Fig. 1, figs. S1 and S2, and table S1). At least one of the age analyses on each crystal was located on the unpolished surface, providing the average age of the most recent ~5 μm of crystal growth [e.g., (*15, 16*)]. Spots located in the polished crystal interiors range in age from 4.6 thousand years to secular equilibrium (>~350 thousand years), and six crystals have at least one interior location that is >51 thousand years. Thus, all crystals except one record growth spanning tens of thousands of years, which is thought to reflect multiple punctuated crystallization intervals [e.g., (*13*)].

[1]Department of Earth and Planetary Sciences, University of California, Davis, Davis, CA 95616, USA. [2]School of Earth and Space Exploration, Arizona State University, Tempe, AZ 85287, USA. [3]College of Earth, Ocean, and Atmospheric Sciences, Oregon State University, Corvallis, OR 97331, USA. [4]Earth Observatory of Singapore, Nanyang Technological University, Singapore. [5]Asian School of the Environment, Nanyang Technological University, Singapore. [6]Department of Geological Sciences, University of Canterbury, Christchurch, New Zealand. [7]Geological and Mining Engineering Sciences, Michigan Technological University, Houghton, MI 49931, USA.
*These authors contributed equally to this work.
†Corresponding author. Email: kmcooper@ucdavis.edu

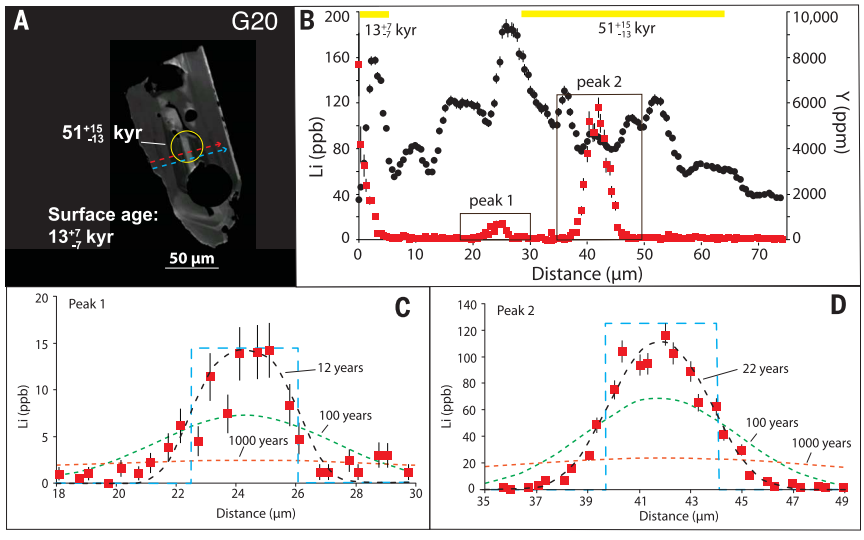

Fig. 1. Lithium and yttrium concentration profiles across zircon crystal G20 and modeling of diffusion of high-Li peaks. (**A**) Cathodoluminescence image of a polished zircon interior with the location of the ^{238}U-^{230}Th age spot shown by the yellow circle. Brightness and contrast have been adjusted uniformly across the image; the unmodified image is available as data S4. The age of the unpolished surface is also indicated. Locations of trace element traverses are shown by red (light elements) and blue (heavy elements) arrows. kyr, thousand years. (**B**) Measured concentrations of Li [red squares, parts per billion (ppb)] and Y [black circles, parts per million (ppm)] in the traverse shown in red in (A). Locations of modeled peaks are shown by labeled black boxes. Yellow bars at the top show the locations along the traverse of age analyses; surface age is shown as a 5-μm region at the rim of the crystal. Error bars, 1σ. (**C** and **D**) Li diffusion profiles for each modeled peak. Red squares represent measured Li concentrations with 1σ Poisson uncertainties (*18*). The modeled initial step function is shown by the dashed blue line, and the modeled diffusion profiles at 700°C are shown as dashed lines for the best-fit diffusion time (black), 100 years (green), and 1000 years (red). All time scales are calculated using diffusion data from (*20*). Other crystals are shown in figs. S1 and S2.

Lithium and other trace element concentration profiles were measured across the same crystals by nanoscale secondary ion mass spectrometry (NanoSIMS) with a spot size of ~0.5 to 1 μm (Fig. 1, figs. S1 and S2, and data S1). These high-spatial-resolution profiles show zones with widths of 5 to 10 μm in which Li concentrations are one to two orders of magnitude higher than in surrounding zones (Fig. 1 and figs. S1 and S2). We considered several potential origins for these peaks in Li concentration, including variations in Li concentrations during zircon crystal growth {due to magma mixing, changes in magmatic vapor [e.g., (*17*)], or enrichment of Li in a boundary layer of melt nearest to the growing crystal face}, diffusion of Li into the rim of an existing zircon crystal, Li migration into the interior of a crystal along fractures, or Li partitioning differences between zones. Diffusion or migration of Li into the crystals after formation would produce profiles with qualitatively different shapes than those observed (fig. S3). Differences in equilibrium partitioning of Li would be predicted to entail covariation of Li with other trace elements, which we do not observe in our data (fig. S4) (*18*). Therefore, we interpret these profiles to reflect diffusional relaxation of concentration variations that originated from changes in melt or magmatic vapor composition during zircon growth (*18*).

Zircon is known for retaining elements such as U and Pb, but diffusion of Li in zircon is comparatively rapid (*19*, *20*). Although coupled diffusion of Li with rare earth elements has been proposed (*21*), we observe no evidence for such coupling in our data (fig. S4), and experimental evidence to date indicates that such coupling does not affect diffusion of Li in zircon (*20*); however, if coupled diffusion were to be documented in future experimental work, our results would need to be reevaluated. To quantify maximum (isothermal) preservation times for the high-Li zones, we modeled the profiles as initial step functions modified by diffusion (*18*). Our calculations yield time scales of years to a few centuries for temperatures of 650° to 750°C (Fig. 2, fig. S4, and table S2). Although isothermal crystal storage is unrealistic, these calculations constrain the maximum time that the crystals could have spent at specific temperatures corresponding to different physical states during storage. For example, none of these crystals could have spent more than a total of ~40 years above the rheological lockup temperature (750°C) or more than a total of ~150 to 1200 years above the solidus (650° to 700°C) (Fig. 2, fig. S5, and table S2) (*18*).

Combining storage time scales from the ^{238}U-^{230}Th crystal ages with diffusion time scales from the Li profiles, we calculated the maximum proportion of its storage time that each zircon crystal could have spent at a specified temperature (Fig. 3). A distinctive aspect of this study is that we can quantify the age of each high-Li zone individually (Fig. 3 and table S3) (*18*). Comparison with the calculated diffusion durations reveals that each crystal (with only one exception: G47) spent <~4% of its storage time (after the formation of high-Li zones) above the solidus (650° to 700°C) and <<1% of this time above the rheological lockup temperature (750°C) (Fig. 3 and table S2). The assumptions made during the diffusion modeling all have the effect of maximizing the calculated diffusion times and percentages (*18*).

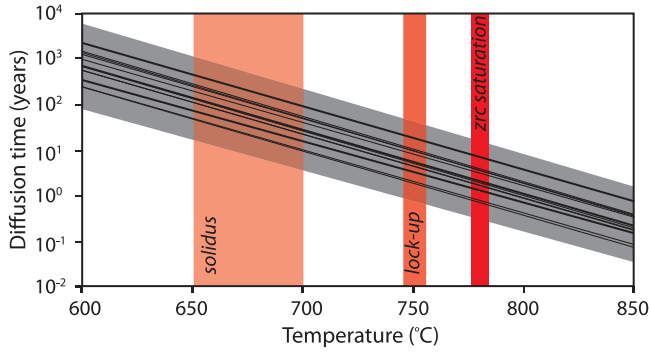

Fig. 2. Diffusion durations as a function of temperature, calculated for all measured peaks. Black lines represent best-fit diffusion durations as a function of temperature (table S2). The gray field encompasses the range of uncertainties in these calculations, which are due to uncertainties in the diffusion coefficient (*20*). Also shown (vertical red-shaded fields) are estimated solidus temperatures, the rheological lockup temperature from Rhyolite-MELTS modeling, and the calculated zircon (zrc) saturation temperature for the Kaharoa rhyolite composition (*18*).

Our data have profound implications for the thermal conditions within the OVC magma reservoir. For example, the data require that these zircon crystals [and likely most of the zircon crystals in the Kaharoa magma (*18*)] were derived from parts of the magma reservoir that were dominantly solid over tens of thousands of years (Fig. 4), in keeping with a protracted history of melt extraction from a cool crystal mush recorded in cumulate plutonic material that was entrained during the Kaharoa eruption (*22*). In addition, our data provide a thermal budget that must be consistent with all of the processes associated with storing and erupting this magma, in that the diffusion modeling constrains the total time that the zircons spent at relatively high temperature. This in turn implies that all heating and cooling related to the crystallization episodes recorded by zircon (including the final assembly and eruption of the magma body) were very rapid (Fig. 4), broadly consistent with previous work suggesting that the Kaharoa eruption resulted from amalgamation of small, isolated magma bodies (*13*, *18*, *23*, *24*).

Furthermore, the duration of subsurface residence of most of the zircon crystals after formation of the high-Li zones spans a time period over which more than 25 OVC eruptions occurred, limiting the possible duration and/or spatial extent of thermal perturbations associated with these eruptions. Importantly, this includes the Rotoiti caldera-forming eruption ~45 thousand years ago (*25*), indicating that this 80 km^3 eruption was not preceded by spatially widespread heating of the magma reservoir over many centuries to millennia.

Our data are consistent with other evidence for cool magma storage (*5*) but contrast with some recent interpretations of coupled Ti-in-zircon crystallization thermometry and ^{238}U-^{230}Th or U-Pb ages, which suggest higher-temperature storage of magmas for tens to hundreds of thousands of years [e.g., (*3, 8*)]. However, we can reconcile our results with these interpretations by considering two points. First, Ti-in-zircon temperatures represent crystallization temperatures, not storage temperatures. Ti-in-zircon crystallization temperatures calculated for the zircons analyzed here [~700° to 825°C; table S1 (*18*)] are much higher than temperatures of long-term storage allowed by our data. Second, many Ti-in-zircon data sets [e.g., (*3, 8, 13*)] show large (>100°C) variations in calculated Ti-in-zircon temperatures in crystals of the same age, rather than showing a systematic, reservoir-wide change in thermal conditions. Intriguingly, when compared at the individual crystal scale, we found a spread of about one order of magnitude in calculated diffusion times for a given temperature (Fig. 2), suggesting that at any one time, there are measurable thermal variations across the reservoir.

Such thermal diversity could also reconcile our results with modeling studies suggesting that liquid-dominated magma bodies may be maintained at high temperatures for hundreds of thousands of years within a larger region of crystal mush [e.g., (*1, 26–28*)]. Our data from individual crystals sample the reservoir at a much finer scale than is tracked in these models. Simple conductive thermal modeling indicates that at a local scale, small tabular bodies (10 to 50 m thick) could cool from 750° to ~650°C in years to decades (fig. S6) (*18*). Coupling these cooling calculations with diffusion modeling indicates an apparent closure temperature for Li diffusion of ~650°C (fig. S6) and diffusion distances for Li that are similar to those observed (*18*). Thus, our data could be explained by rapidly cooling small bodies of melt to ~650°C and maintaining them at or below that temperature within a broader reservoir with a higher average temperature (Fig. 4), as numerical models suggest. This explanation is also consistent with shear velocity evidence for a complex of sills beneath a similar volcano, Toba (*29*). Our data do not preclude the presence of hotter regions or even

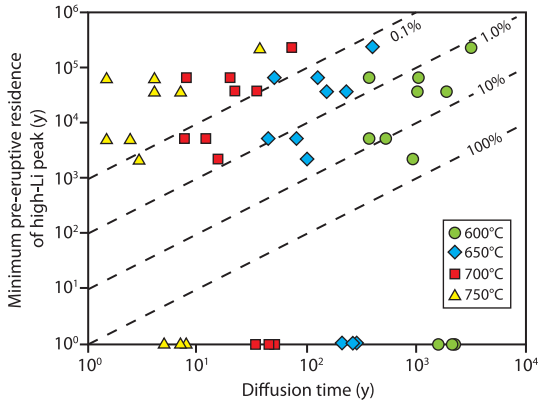

Fig. 3. Comparison of pre-eruptive residence of high-Li peaks with modeled diffusion durations for the same peaks. Minimum pre-eruptive residence durations of high-Li peaks were calculated from the minimum zircon interior age (within analytical error) minus the eruption age for peaks that overlapped with age spots, and from minimum surface ages minus the eruption age for peaks that did not overlap with interior age spots (table S2) (*18*). In the case of three peaks from two crystals, minimum ages were within error of eruption age; diffusion time scales for these are shown along the *x* axis. Diffusion time scales for each peak are shown at modeled temperatures of 600°C (green circles), 650°C (blue diamonds), 700°C (red squares), and 750°C (yellow triangles). The diagram is contoured (dashed lines) for the percentage of the pre-eruptive residence time that is represented by the diffusion time scales. y, years.

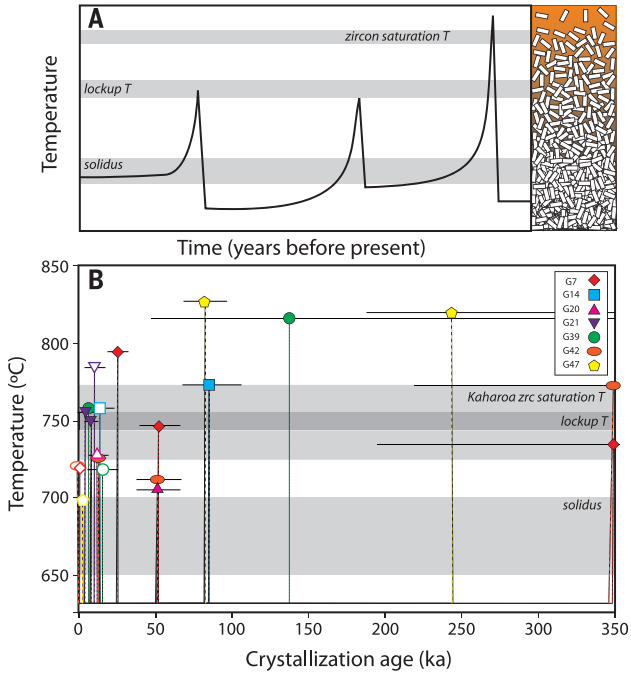

Fig. 4. Thermal histories for the Kaharoa zircons. (**A**) Schematic diagram showing thermal evolution of a magma reservoir recorded in crystals. The black line shows a schematic thermal history in which a region where a zircon crystal is growing is heated and cooled multiple times before eruption. The width of the curve above any given temperature (*T*) represents the duration of time that the crystal spends above that temperature (exaggerated in this schematic for ease of visibility). A schematic of the crystallinity of the reservoir with temperature is shown at the right. (**B**) Time-temperature history recorded in the zircon crystals from this study. Each crystal is represented by a different symbol (open symbols represent surface analyses), and all measured ^{238}U-^{230}Th ages are plotted with their 1σ uncertainties at the corresponding Ti-in-zircon temperature. Points yielding ^{238}U-^{230}Th activity ratios within error of secular equilibrium are plotted at 350 thousand years ago (ka). The number of temperature spikes shown corresponds to the number of age analyses, representing a minimum number of growth events, assuming growth was not continuous. The widths of the peaks in temperature correspond to the diffusion durations (within the resolution of the line widths), and the temperature between peaks is arbitrarily set below the lowest recorded crystallization temperature. The gray shaded regions indicate the range of zircon saturation temperatures for the Kaharoa eruption, the estimated rheological lockup temperature, and the solidus temperature (*18*).

a small, persistent, dominantly liquid magma body, as long as these were thermally isolated from the storage location of the analyzed zircon crystals. The near-solidus bodies hosting these zircon crystals could represent the cooler areas of the reservoir, which are remobilized rapidly (*30*, *31*) immediately before eruption by injection of new crystal-poor magma. Whether similar thermal histories are common for zircon in larger eruptions requires further study. Our approach represents an exciting avenue of research to develop a more detailed understanding of thermal conditions of magma storage and, through the thermal and chemical changes recorded in the crystals, to understand the processes of mass and heat input to and output from magma reservoirs.

REFERENCES AND NOTES

1. C. Annen, *Earth Planet. Sci. Lett.* **284**, 409–416 (2009).
2. O. Bachmann, G. W. Bergantz, *J. Petrol.* **45**, 1565–1582 (2004).
3. M. Barboni *et al.*, *Proc. Natl. Acad. Sci. U.S.A.* **113**, 13959–13964 (2016).
4. A. Burgisser, G. W. Bergantz, *Nature* **471**, 212–215 (2011).
5. K. M. Cooper, A. J. R. Kent, *Nature* **506**, 480–483 (2014).
6. A. Halliday *et al.*, *Earth Planet. Sci. Lett.* **94**, 274–290 (1989).
7. H. E. Huppert, R. S. J. Sparks, *J. Petrol.* **29**, 599–624 (1988).
8. J. F. Kaiser, S. de Silva, A. K. Schmitt, R. Economos, M. Sunagua, *Earth Planet. Sci. Lett.* **457**, 73–86 (2017).
9. G. A. Mahood, *Earth Planet. Sci. Lett.* **99**, 395–399 (1990).
10. W. Degruyter, C. Huber, *Earth Planet. Sci. Lett.* **403**, 117–130 (2014).
11. E. W. Klemetti, C. D. Deering, K. M. Cooper, S. M. Roeske, *Earth Planet. Sci. Lett.* **305**, 185–194 (2011).
12. A. Rubin *et al.*, *Contrib. Mineral. Petrol.* **171**, 1–18 (2016).
13. S. Storm, A. K. Schmitt, P. Shane, J. M. Lindsay, *Contrib. Mineral. Petrol.* **167**, 1000 (2014).
14. C. J. N. Wilson, D. M. Gravley, G. S. Leonard, J. V. Rowland, in *Studies in Volcanology: The Legacy of George Walker*, T. Thordarson, S. Self, G. Larsen, S. K. Rowland, A. Höskuldsson, Eds. (International Association of Volcanology and Chemistry of the Earth's Interior Special Publication 2, Geological Society of London, 2009), pp. 225–247.
15. A. K. Schmitt *et al.*, *Contrib. Mineral. Petrol.* **162**, 1215–1231 (2011).
16. J. A. Vazquez, M. I. Lidzbarski, *Earth Planet. Sci. Lett.* **357**, 54–67 (2012).
17. A. J. R. Kent *et al.*, *Geology* **35**, 231–234 (2007).
18. Materials and methods are available as supplementary materials.
19. D. J. Cherniak, E. B. Watson, *Contrib. Mineral. Petrol.* **160**, 383–390 (2010).
20. D. Trail *et al.*, *Contrib. Mineral. Petrol.* **171**, 25 (2016).
21. T. Ushikubo *et al.*, *Earth Planet. Sci. Lett.* **272**, 666–676 (2008).
22. K. Graeter, R. Beane, C. Deering, O. Bachmann, D. Gravley, *Am. Mineral.* **100**, 1778–1789 (2015).
23. P. Shane, S. Storm, A. K. Schmitt, J. M. Lindsay, *Lithos* **140**, 1–10 (2012).
24. J. W. Cole *et al.*, *Earth Sci. Rev.* **128**, 1–17 (2014).
25. M. Danisik *et al.*, *Earth Planet. Sci. Lett.* **349**, 240–250 (2012).
26. C. Annen, J. D. Blundy, J. Leuthold, S. J. Sparks, *Lithos* **230**, 206–221 (2015).
27. L. Caricchi, G. Simpson, U. Schaltegger, *Nature* **511**, 457–461 (2014).
28. S. E. Gelman, F. J. Gutierrez, O. Bachmann, *Geology* **41**, 759–762 (2013).
29. K. Jaxybulatov *et al.*, *Science* **346**, 617–619 (2014).
30. G. W. Bergantz, J. M. Schleicher, A. Burgisser, *Nat. Geosci.* **8**, 793–796 (2015).
31. J. M. Schleicher, G. W. Bergantz, R. E. Breidenthal, A. Burgisser, *Geophys. Res. Lett.* **43**, 1543–1550 (2016).

ACKNOWLEDGMENTS

The full data set for this paper is available in tables S1 to S3 and data S1. We thank C. Hitzman for developing Li analytical protocols for the NanoSIMS instrument at Stanford University and for assistance with running analyses. The Arizona State University (ASU) facility is supported by NSF awards ARRA-960334 and EAR-1352996, and support for the ASU analyses was provided by the facility. This work was partially supported by NSF awards EAR-1144945 and EAR-1426858 to K.M.C. and EAR-1425491 to A.J.R.K. and by Singapore Ministry of Education grant MoE2014-T2-2-041 to F.C.

SUPPLEMENTARY MATERIALS

www.sciencemag.org/content/356/6343/1154/suppl/DC1
Materials and Methods
Supplementary Text
Figs. S1 to S6
Tables S1 to S3
References (*32*–*52*)
Data S1 to S8

27 January 2017; accepted 18 May 2017
10.1126/science.aam8720

Science

Rapid cooling and cold storage in a silicic magma reservoir recorded in individual crystals

Allison E. Rubin, Kari M. Cooper, Christy B. Till, Adam J. R. Kent, Fidel Costa, Maitrayee Bose, Darren Gravley, Chad Deering and Jim Cole

Science **356** (6343), 1154-1156.
DOI: 10.1126/science.aam8720

Quick eruption after a long bake

Minerals such as zircon can record the storage conditions of magma before volcanic eruption. Rubin *et al.* combined traditional ^{238}U-^{230}Th dating with lithium concentration profiles in seven zircons from the Taupo supervolcanic complex in New Zealand to determine magma storage conditions. The zircons spent more than 90% of their lifetime in an uneruptible, mostly crystalline, and deep magmatic reservoir. The zircons were eventually transported to hotter, shallower, and eruptible magma bodies, where they spent only decades to hundreds of years before eruption. The result suggests a two-stage model for magmatic systems with large thermal variations.

Science, this issue p. 1154